HyGage: Solving the Hysteresis Puzzle with a New Streamflow Monitoring Method

Marian Muste[1], Kyeongdong Kim[1], Alexandre Hauet[2], Christophe Rousseau[2], Emma House[3], Ehab Meselhe[3], Ibrahim Demir[3]

[1]IIHR-Hydroscience & Engineering, The University of Iowa, Iowa City, IA, USA

[2]Institut des Géosciences de l'Environnement (IGE) - Équipe Hydrimz, Université Grenoble Alpes, Grenoble, France

[3]Department of River-Coastal Science and Engineering, School of Science and Engineering, Tulane University, New Orleans, LA, USA

Abstract

The questionable reliability of discharges obtained using the traditional stage–discharge method under gradually varied flow conditions continues to motivate the search for improved monitoring approaches that support water resources management, streamflow forecasting, and multipurpose scientific investigations related to the water cycle. This paper introduces HyGage, a new physically based monitoring method grounded in the governing equations of spatiotemporal, gradually varied, shallow open channel flow. The methodology integrates measurement elements commonly employed in the index velocity and slope area methods within a unified analytical framework, enabling real time discharge estimation in both steady and gradually varied flows without relying on the semi empirical techniques of the past. The performance of HyGage is evaluated by comparing its discharge estimates with those obtained from established methods. Unlike conventional approaches, HyGage is not built around any specific instrument; instead, it can flexibly incorporate combinations of immersed, close range, and remote sensing measurements through seamless integration.

Keywords: gradually-varied flows, streamflow monitoring, stage-discharge rating, index-velocity method, slope-area method, hybrid gaging method (HyGage)

Introduction

The automated monitoring of flow rates in rivers is the result of more than a century-long development with the goal of supporting observations and investigations on the water cycle for a myriad of practical and scientific uses. The oldest streamflow monitoring method is the stage-discharge rating curve (labeled herein HQRC) which continues to be widely used worldwide because it is easier to install and operate compared to other approaches. The major HQRC limitation is the time-wise, quasi-steady flow assumption applied uniformly for observing flows using a single hydraulic variable, the flow depth. The flow depth is typically derived from the measurement of water surface level (a.k.a. stage) from a local gage datum. The HQRC performance is totally acceptable for quasi steady and uniform flows, conditions that are attained between precipitation events when the river is at its base flow. The base flow persistence in perennial rivers is directly related to the climatic and hydrological settings of the monitoring site. Most of the monitoring sites located in temperate and continental climates are exposed to slow evolving, sporadic spatial changes of river morphology and shorter and more frequent temporal changes in the flow regimes triggered by precipitation events passing through the station.

The large-scale (stream-reach) morphological changes are produced by processes that mainly affect the longitudinal river profile (e.g., migration, avulsion, vegetation growth). There are also local (cross-sectional) morphological changes that occur in the vicinity of a river gaging site (e.g., erosion, deposition, bank failure). The natural morphological changes are often compounded with those produced by man-made hydraulic structures installed in the stream (e.g., locks, dams, bridge abutments). The presence of morphological changes downstream the station leads to steady and non-uniform flows, resulting in flow storage in the stream reach. The stream-reach and cross-sectional morphological changes can act simultaneously making their detection complex and costly due to the need for recursive gaging site inspections (Darienzo et al., 2021). Morphological changes at any scale can modify or even shift the hydraulic regimes at the station (e.g., changing the flow control from channel to local) and/or create areas of backwater that affect the validity of the originally constructed ratings (Herschy, 2009). Temporal changes in the flow regimes at a station are produced by runoff entering the stream or changes in the operation regimes at upstream installed hydraulic structures. These flow transitions produce unsteady and non-uniform flows over the whole duration of the transition (a.k.a. fluvial wave period).

For the present context, we label the spatial-temporal changes occurring at a gaging station by the term of Spatial-Temporal Gradually Varied Flow (ST-GVF). This broader definition includes unsteady, non-uniform open channel flows that gradually modify the water surface profile in the vicinity of the gaging station. These flows are not directly accounted for by the current conventional monitoring protocols based on stage, index-velocity, or free slope measurements because these methods assume the perpetuity of the time-wise, quasi-steady flow. This assumption does not distinguish between the different flow mechanisms on the rising and falling limbs of the hydrographs during ST-GVFs and those acting during steady flows (Muste et al., 2025b).

Propagation of ST-GVFs through gaging stations often involves both flow storage and flow unsteadiness in the vicinity of the measurement site (Rantz et al., 1982; Dykstra & Dzwonkowski, 2020). These flow variations give rise to hysteretic behavior in the stream. Hysteresis is a nonlinear process in which the state of the system depends not only on its current input but also on the sequence of prior conditions that led to that state (Prowse, 1984). In open-channel flows, hysteresis driven by spatiotemporal variability is pervasive, frequent, and persistent. Backwater effects can influence the full range of discharges, while unsteady flows in temperate-climate inland rivers often account for more than 50% of annual flow conditions (Muste et al., 2025a). Hysteresis also appears in other fields—such as magnetism, electrical systems, and mechanical systems—and can be characterized mathematically for deterministic signals (Ikhouane, 2013) or analytically when the governing physical laws are known.

The simple HQRC method is the least sensitive method to ST-GVF-induced hysteresis as it traces the flows through a one-to one stage-discharge relationship. The intrinsic mechanics of ST-GVFs leads to non-unique, hysteretic relationships between any pair of hydraulic variables, especially when high magnitude and flashy hydrologic events occur in low-land rivers (Dottori et al., 2009; Muste et al., 2020; Muste et al., 2025a). Continuing to overlook the hysteretic behavior of hydraulic variables during unsteady flows epitomizes a departure from our knowledge of the physical processes underlining open-channel hydraulics resulting in epistemic uncertainties (Schmidt, 2002; Beven, 2016). Epistemic uncertainties compound other sources of streamflow-monitoring error (Baldassarre & Montanari, 2009; Westerberg & Karlsen, 2024), rendering data unreliable, especially during extreme flows (Dottori et al., 2018; Kreibich et al., 2022) when the accuracy of data is of outmost importance (McMilan et al., 2017).

Streamflow monitoring agencies are aware of the limitations of the HQRC data acquired in real time and have tackled ST-GVF regime changes by developing correction methods based on additional ratings, analytical corrections, or making recourse to numerical simulations. The first HQRC corrections methods for ST-GVF presence were developed for unsteady flows by Jones (Jones, 1915) with subsequent refinements brought, among others, by Boyer (1937); Henderson (1966), Fenton & Keller (2001), Petersen-Øverleir (2006), and Schmidt & Yen (2009). Customized HQRC correction methods were developed to tackle steady, non-uniform flows produced by local gage controls (e.g., Arico et al., 2008; Dottori et al., 2009). HQRC correction methods have been also developed to adapt ratings to the morphological changes occurring in the station vicinity (Schmidt & Garcia, 2003; Mansanarez et al, 2019). The above-mentioned HQRC corrections are only rarely and non-uniformly applied in real time due to the additional costs they incur and because of the lack of convincing cost-benefit analysis documenting the improvements brought by corrections. Consequently, most HQRC gaging stations in the US refer to the real time data as "provisional' until they are verified for shifts ratings caused by morphological changes and corrections for unsteadiness and backwater effects (USGS, 2010). After periodic reviews (typically at 6-month interval) the data are labeled as "final" and considered that have accounted for the mix of all overlooked processes in real-time reporting.

The limited availability of systematic experimental evidence on the severity of hysteretic effects in natural streams, coupled with the substantial cost and effort required to document these effects comprehensively, has resulted in a status quo in which HQRC in ST-GVFs often remains unaddressed. This inaction can markedly degrade data accuracy, especially when real-time data is needed at sub-daily sampling intervals (Beven, 2006; Holmes, 2016). Recognizing these limitations, monitoring agencies have sought to improve the reliability of discharge estimation by testing and implementing alternative approaches, such as the index-velocity method (IVRC) and the continuous slope-area method (CSA). The development and adoption of these methods have been facilitated by advances in measurement technologies since the 1980s—particularly the emergence of acoustic sensing instruments (Laenen, 1985; ISO 1070:1992 - superseded by ISO 1071:2018). Nevertheless, comprehensive evaluations of HQRC-based corrections, IVRC, and CSA methods remain ongoing, as their comparative performance continues to be critically examined (e.g., Muste et al., 2025b).

Motivated by the current challenges in streamflow monitoring, especially during flash floods, and the increased availability of new measurement technologies such as acoustic, radar, image velocimetry (Tsubaki et al., 2025; Sermet and Demir, 2023), we assembled a new hybrid monitoring method labeled HyGage (Muste at al., 2023) protected by a patent application (USPTO, 2026). The method is grounded in Saint-Venant equations (SVE) applied with strict observation on its assumptions (Saint-Venant, 1871; Chow, 1959). Coincidentally, the SVE assumptions are fulfilled if the gaging site location is selected using the best practice guidance (Rantz et a., 1982). The SVE have proven their reliability to accurately capture ST-GVFs even for situations where slight morphological channel changes occur (Litrico & Fromion, 2009; Yu et al., 2020). The HyGage theoretical background is applied in conjunction with directly measured hydraulic variables and spatiotemporal gradients acquired with combinations of contemporary instruments tested in conjunction with the IVRC and CSA methods without making recourse to ratings.

The paper first presents an overview of the IVRC and CSA method components integrated into the HyGage approach, with reference to the instrumentation deployed at the benchmark gaging station located in Grenoble on the Isère River (France). It then describes the conceptual foundation of HyGage method and, for the first time, demonstrates its implementation using a customized instrumentation layout installed at the Clear Creek gaging station in Oxford, Iowa (USA). Finally, we show how HyGage reduces key conceptual uncertainties inherent in conventional monitoring practices and highlight the new opportunities enabled by its adoption.

METHODS

General Considerations

This section emphasizes the conceptual foundations of the HyGage approach and its first implementation for monitoring ST-GVFs at an operational gaging site. The HyGage concept draws inspiration from and integrates in an innovative manner, measurement components of the IVRC and CSA methods. HyGage development was motivated by a growing body of observational evidence from IVRC and CSA stations, as these data sets showed that augmenting traditional stage measurements—which describe the geometric state of channel flow—with additional hydraulic variables such as index velocity or free-surface slope provides a more realistic representation of flow dynamics compared with the steady HQRC method. This enriched description has been shown to improve the accuracy of monitored discharge and enhance the predictive capability for ST-GVF forecasting (Muste et al., 2019; 2022a; 2022b).

In this paper, we designate the HQRC, IVRC and CSA methods as conventional as they have been already well defined, proof-tested, and fully documented (Kennedy, 1984 for HQRC:

Levesque & Oberg, 2012 for IVRC; and Smith et al., 2010 for CSA). The description in this section assume the familiarity of the readers with the basic procedure of each of these methods. As most of the streamflow data is acquired with the century-old HQRC method, we provide essential features to place it in the paper context. In essence, HQRC development relies on indirect, semi-empirical procedures in which simultaneous measurements of discharge and stage are paired using a graphical approach (Kennedy, 1984). The final form of the HQRC—commonly referred to as the rating curve—is then shaped using statistical techniques, which are in some cases only weakly justified, and supplemented by expert judgment (Fenton, 2018; Rozos et al., 2022). Once established, the ratings are used to convert real-time stage data into corresponding discharge estimates.

Given that the IVRC, CSA, and HyGage methods can be implemented using diverse sensing technologies and deployment configurations, this section illustrates their practical application at two gaging sites: the Grenoble Campus station on the Isère River (Gières, France) and the Oxford station on Clear Creek (Iowa, USA). Additional details about these stations are provided in Section 3. Both locations were initially equipped for the traditional HQRC method, placing them firmly within globally standardized streamflow monitoring practices. They offer unique experimental value because, to the authors' knowledge, there are very few—if any—sites worldwide where HQRC, IVRC, and CSA approaches have been deployed simultaneously. This co-location of monitoring strategies makes the Grenoble Campus and Oxford sites particularly well suited for testing both individual HyGage components and the fully integrated HyGage framework. Among the two, the Oxford test site is especially significant for HyGage presentation: it is the only location that includes direct measurements of all required hydraulic inputs using best-practice instrumentation layouts. The site was intentionally designed to support a comprehensive evaluation of the HyGage concept and its operational elements, as discussed in subsequent sections.

IVRC implementation

The IVRC implementation at Grenoble-Campus and Oxford sites are similar but accomplished with different set of instruments. For Grenoble-Campus station used here for exemplification, the IVRC rating is obtained by simultaneous measurements of index-velocity acquired with a horizontal Acoustic Doppler Current Profiler (H-ADCP) installed on the riverbank and ADCP transects acquired close to the H-ADCP location. There are about 130 ADCP measurements available for analysis covering the entire range of flows as this station. The abundance of ADCP data for this site is related to the station's role in benchmarking various monitoring alternatives (Rousseau & Barthelemy, 2025).

A first step in developing the IVRC rating is to assess the quality of the H-ADCP (a.k.a. Side Looker or, for brevity, SL) velocities acquired along the instrument acoustic path with ADCP velocities acquired from transects over the overlapping area, as illustrated in Fig. 1a. Specifically, SL in-bin measurements acquired over 1m long segments (containing 20 bins) along the instrument path are compared with in-bin ADCP measurements in 1m x 0.1m areas along the SL measurement path. The SL raw data was averaged over ΔT_{SL} = 10 min, while the ADCP data was averaged for ΔT_{ADCP} = 10 min. The SL-ADCP data comparison is made for ADCP transects acquired on the rising limb of the hydrographs at WSE = 208.9 m

(A), 209.4 m (B) and WSE = 210.6 m (C) shown in Fig. 1b. These water elevations correspond to discharges of 88.3 $m^3 s^{-1}$, 144.3 $m^3 s^{-1}$, 303.2 $m^3 s^{-1}$, respectively. The cross-sectional distributions of the streamwise velocity component measured by ADCP and the velocity profiles acquired with SL and ADCP in the overlapping areas for the stages A, B, and C are illustrated in Figures 1c1-1c2, 1d1-1d2, and, 1e1-1e2, respectively.

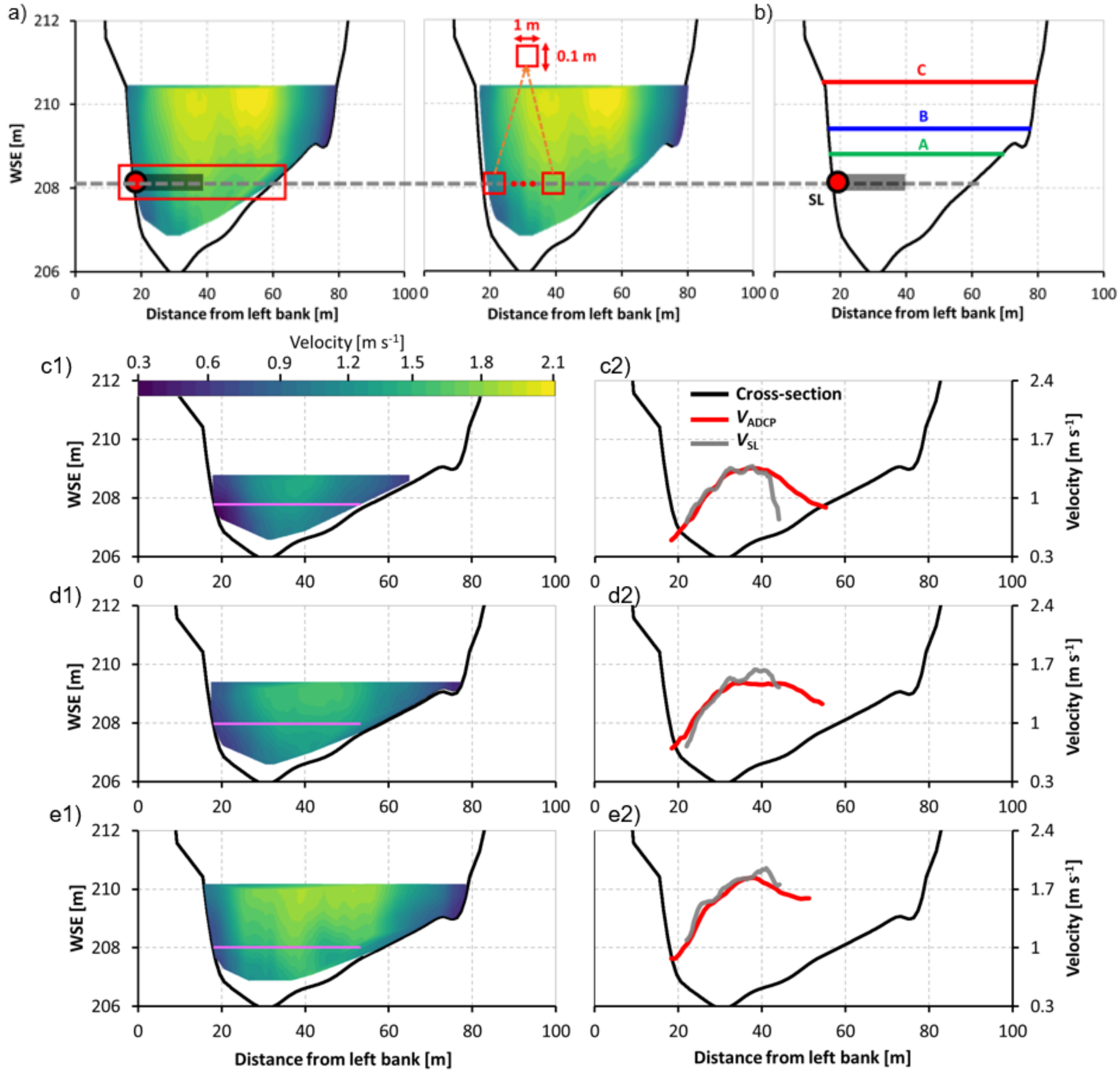

Figure 1. Comparison of simultaneous HADCP (SL) and ADCP measurements: a) layout of the overlapping areas; b) stages used for SL - ADCP comparison: *WSE* = 208.9 m (A), *WSE* = 209.4 m (B), and *WSE* = 210.6 m (C); 1c1, 1c2) comparison of SL-ADCP for stage A; 1d1, 1d2 same comparison for a stage B; 1e1, 1e2 same comparison for stage C.

Collectively, the SL-ADCP data comparisons for all tested stages display a remarkable good agreement for the near-field area of the SL acoustic path and a gradual increase in differences in the far-field area (i.e., distances larger than 40 m from the riverbank). The reliability of the SL in the far-field is affected by multiple potential causes that have been signaled and evaluated in previous studies (Le Coz et al., 2008; Hidayat et al., 2011). The persistence of these findings in various SL deployments and flow situations suggests that the quality assessment conducted above is a necessary step before initiating the construction of the IVRC rating. For the present study we use only SL readings in SL-ADCP agreement area, i.e., from the first valid SL bin to the bin located at 40m.

The SL data curated as shown above in conjunction with the large dataset of ADCP transects available at this gaging station allowed to develop a composite IVRC rating that is function not only on the index velocity but also accounting for specific stage ranges, as illustrated in Figure 2a. The multi-parameter regression for determining the IVRC rating is similar with the approach used by Levesque & Oberg (2012) for constructing the V_{index} - V_{mean} relationship for real-time monitoring.

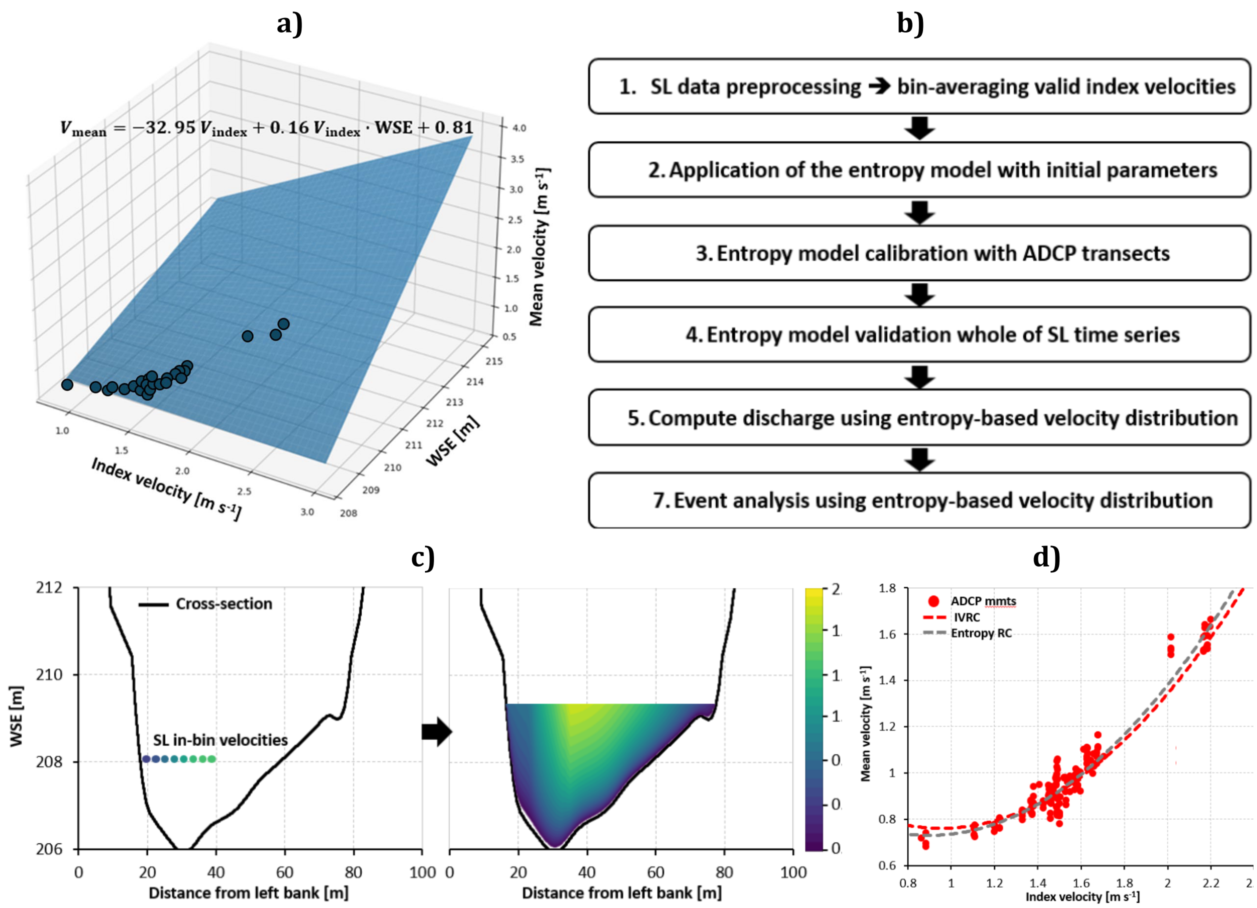

Figure 2. Alternative approaches to relate V_{index} - V_{mean} for supporting the IVRC method implementation: a) conventional approach (Levesque & Oberg, 2012); b) entropy model applied to SL datasets; and c) reconstruction of the cross-sectional distribution of the streamwise velocity using the entropy model with SL input; and d) comparison of the two IVRC implementation approaches.

Having in mind the fully analytical implementation of HyGage protocol (i.e., without requiring constructions of ratings), we developed an alternative approach for determining the V_{index} - V_{mean} relationship based on the entropy theory. The entropy principle is a generic stochastic theory applicable to a wide range of hydrological systems (Singh, 2025). This concept was introduced in riverine environment by Chiu (1988; 1989) and subsequently optimized by Moramarco et al. (2004, 2017) to accommodate various approaches for index-velocity measurement. This alternative approach to conventional construction of the IVRC rating has been consistently found to reasonably estimate the cross-sectional mean velocity distribution in normal and upper flow ranges without requiring the extensive velocity datasets. Regardless of the approach used for IVRC implementation, the cross-sectional area must be expressed as a function of stage to determine the discharge (Levesque & Oberg, 2012). Repetition of the cross-section surveys is considered good practice to observe possible changes in the station morphology (Kennedy, 1984).

For this study, we developed a software package in conjunction with SL measurements and ADCP calibration/validation data acquired at Grenoble-Campus (Kim et al., 2025). The main software steps for our entropy model are graphed in Fig. 2b. The model was trained using 6 ADCP measurements in contrast with the 122 ADCP measurements used for developing the IVRC rating with the conventional approach. The cross-sectional streamwise velocity distribution derived by our entropy model is illustrated in Fig. 2c. The IVRC ratings obtained with the two implementation alternatives are shown in Figure 2d. While differences less than 5% between the ratings are visible for the lowest and highest flow ranges, there is good overall agreement between the IVRC approaches indicating that the entropy mode is an efficient procedure for obtaining the V_{index} - V_{mean} relationship with just of fraction of the calibration data.

CSA Implementation

The detailed description of the slope-area method is provided in Dalrymple & Benson (1967) and will be not reiterated here. In short, the method implementation requires a cross-section survey and measurement of free-surface slope at several successive locations along the stream. The river stages can be measured independently with a variety of instruments (e.g., Sauer & Turnipseed, 2010). Notable, currently the CSA method gains increased attention through the measurement of FSS from remote sensing (Bauer-Gottwein et al., 2024; Schwatke et al., 2024; Wang et al., 2025) which is particularly relevant for implementation of the HyGage method.

In this paper, the CSA method is applied for both Grenoble-Campus and Oxford sites. Ideally, the CSA method should be implemented with three or more stage measurements acquired over a short distance, i.e., less than 500m for a medium size river (House et al., 2025b). The constraint on the distance is similar with the spatial discretization used in numerical simulations that fulfils the SVE assumption for avoiding significant discharge changes through the cross sections defining the computational reach (House et al., 2025). The shortest available distance for determining FSS at Grenoble-Campus is 1,270 m which contrasts with the 187m span set for the Oxford station. While the spacing is not an optimal for Grenoble-Campus site, the approx. 1km distance between the stage measurement points is one order of magnitude smaller than 10 to 30 km distances typically used for calculation of the FSS in previous studies (e.g., Dottori et al., 2009). The CSA discharges, Q_{CSA}, are determined using protocols tested in previous studies (Muste et al., 2019). The bed slope, S_0, and Manning roughness coefficient, n_0, estimation for the sites is conducted with protocols described in Lamoreaux et al. (2025). For this analysis, S_0 and n_0, were kept constant with the values reported in Tab.1.

HyGage Monitoring Concept

The HyGage method featured in this paper is a physically-based monitoring approach that takes advantage of the progress made over multiple decades in observing streamflow time series with various measurement concepts and instruments. The central paradigm shift of this method entails the use of the Saint-Venant equations for monitoring both steady uniform and ST-GVF flows instead of making recourse to semi-empirical relationships based on the quasi-steady uniform flows assumption. An intuitive form of the Saint-Venant equations (SVE) for monitoring purposes is its non-conservative version provided by Eq. (1) that relates the steady uniform discharge, Q_0, (obtained herein via Manning equation) with the unsteady, non-uniform discharge, Q, stemming from various ST-GVF regimes (e.g., Henderson, 1966).

$$Q = Q_0 \sqrt{1 - \frac{1}{S_0}\frac{\partial h}{\partial x} - \frac{V}{gS_0}\frac{\partial V}{\partial x} - \frac{1}{gS_0}\frac{\partial V}{\partial t}} \tag{1}$$

[steady uniform ---→]
[steady non-uniform (gradually varied) ----------→]
[unsteady non-uniform (spatial-temporal gradually varied) →]

where variables *h* (depth) and *V* (cross-sectional velocity), the spatiotemporal gradients appearing in the last three terms of the equation along with the Manning's roughness coefficient, *n*, the bed slope, S_0, and the geometry of the cross section where the discharge is calculated. The number of terms on the right side of SVE is associated with the type of fluvial wave propagating through the observation point (Henderson, 1966): kinematic (first term), diffusive (first three terms), fully dynamic (all terms). More specifically, the kinematic wave accounts only for friction and gravity forces, the diffusive wave appends the pressure force, while the fully dynamic wave also includes the local acceleration forces. Notable, the SVE implicitly accounts for morphological changes at the station through the pressure and convective terms in Eq. (1).

The change in signs of the variable derivatives on the rising and falling limbs of the hydrograph in Eq. (1) leads to hysteretic (non-unique) relationships between any pair of ST-GVF hydraulic variables (i.e., free-surface slope - *FSS*, velocity - *V*, and Water Surface Elevation - *WSE*). The departure of these hysteretic relationships from the unique HQRC function for steady and uniform flow (Q_0) are visualized as loops in the relationships between pairs of hydraulic variables and phase lags between the peaks of the variable hydrographs (Muste et al., 2025a). The variable peak phasing progresses strictly in the following order: *FSS*, *V*, *Q*, and *WSE*. The hysteresis severity (indicated by the degree of departure of the non-unique relationships from the unique rating curves) is different for each site and propagating event. Broadly speaking, while hysteresis is intrinsically present in all forms of ST-GVFs, its severity can be mainly related to (Moussa & Bocquillon, 1966; Ferrick, 1985; Perumal et al., 2006; Moramarco et al., 2008; Perret et al., 2022):

- Channel bed slope (low slopes are often leading to severe hysteresis)
- Flow magnitude and flashiness (high, sharp hydrographs produce severe hysteresis).
- Froude # (for $Fr \ll 1$ severe hysteresis; for $Fr < 1$ moderate, and for $Fr > 1$, negligible).

Directly determining discharge with Eq. (1) requires continuous direct measurements of the primitive hydraulic variables h and V and of the spatial-temporal gradients appearing in the last three terms of the equation. The flow depth, h, is usually derived from the measurement of stage (WSE). The H value is not necessarily zero when the effective flow depth is zero. The derivative ($\partial h/\partial x$) is the free-surface slope (FSS) estimated over a distance commensurate with the wavelength of the propagating fluvial wave (House et al., 2025a). Selecting longer river reach lengths departs from the scales of the SVE discretization that are strictly valid for elementary flow volumes. We deem that, similar to Petersen-Øverleir (2006) finding, the HyGage monitoring concept is applicable for situations where changes in channel geometry and resistance are relatively small during ST-GVFs, i.e., of the same order of magnitude as the discharge measurement uncertainty. If this is not the case, further segmentation is needed over time-periods and space-intervals when the flow control can be considered closer to stable (House et al., 2025a).

One of the most difficult tasks in applying Eq. (1) in practice is to determine FSS over short distances in the vicinity of the station because its estimation depends on instrument resolution and accuracy, as well as on the bed slope and event magnitude (e.g., WSDOT, 2025). However, studies showed that modern instruments are capable to capture free-surface slopes over distances of tenth of meters (Smith et al. 2010; Muste et al. 2025b). Another difficult task is to analytically convert the index velocity (V_{index}) into bulk flow velocity (V) instead of using empirical ratings as currently done for IVRC method. This task is still under research, with some successful attempts demonstrated in prior works (Le Coz et al., 2008; Nihei & Kimizu, 2008: Hoitink et al. 2018; Johnson & Cohen, 2017; and Fenton, 2025). In this paper we tackle the V_{index} to V conversion with the entropy concept, discussed in the previous section. Overcoming the above-mentioned difficulties allows for application of Eq. (1) fully analytically without additional restrictive assumptions.

In order to demonstrate the impact of directly measuring all or only some of the terms in the SVE to capture the actual ST-GVF features, we made recourse to numerical simulations carried out with 1-D unsteady HEC-RAS applied to a hysteretic site investigated through several prior studies (Muste et al., 2022a, 2022b; House et al., 2025a, 2025b; Muste et al, 2025a). Fig. 3 replicates hysteretic features simulated for a large flood wave propagating through a 300m-long reach downstream from the USGS station # 0555830 at Henry on Illinois River (IL, USA). The event simulation allows to readily represent the discharge time series, labeled Q_{HyGage} (Dyn), accounting for all the SVE terms in Eq. (1) - similar to what HyGage would measure - as well as discharges provided by a hypothetical CSA monitoring, Q_{CSA} (Diff), obtained by retaining only the $\partial h/\partial x$ term in the summation. The plots in Fig. 3 also contain datasets provided by the IVRC method, Q_{IVRC} (semi-empirical), as reported by USGS who maintains and operates and IVRC at this site. The switch from a prior HQRC, labeled Q_{HQRC} (Q_0), to IVRC for this site was triggered by repeated instances when flow measurements with the HQRC method were deemed inaccurate. Finally, Fig. 3 includes the HQRC data corrected with the Fread (1975) algorithm, Q_{FRE} (Q_0) for illustrating the performance of one of the correction methods applied to HQRC (see Muste et al., 2025b for the analysis of the performance of more HQRC correction methods).

Given that there are no direct discharge measurements for this 1.5-month event (a daunting task itself), we cannot conclude on the most reliable of the five methods illustrated in Fig. 3. However, relatively speaking, it is apparent that the hysteretic loops and the time series offered by the simulated HyGage and CSA methods are in close agreement while the HQRC datasets corrected with the Fread method and the IVRC datasets are slightly off. It is quite apparent that the simple stage-discharge (HQRC) method completely overlooks the dynamics of the flow propagation. Numerical simulations replicating this event illustrate that the uncertainty in the HQRC discharge can reach significant differences from the actual flows in the area of the maximum loop size for same stages on the rising and falling limbs of the hydrograph. Also notable is that discharge hydrographs for the HyGage, CSA, IVRC and Fread methods plotted in Fig. 3 are peaking at higher values and occur prior to the timing of the discharge peak of the HQRC. The hysteretic features illustrated in Fig. 3 are akin to those found through multiple prior studies at a variety of sites conducted by these authors (Muste et al., 2025a; 2025b).

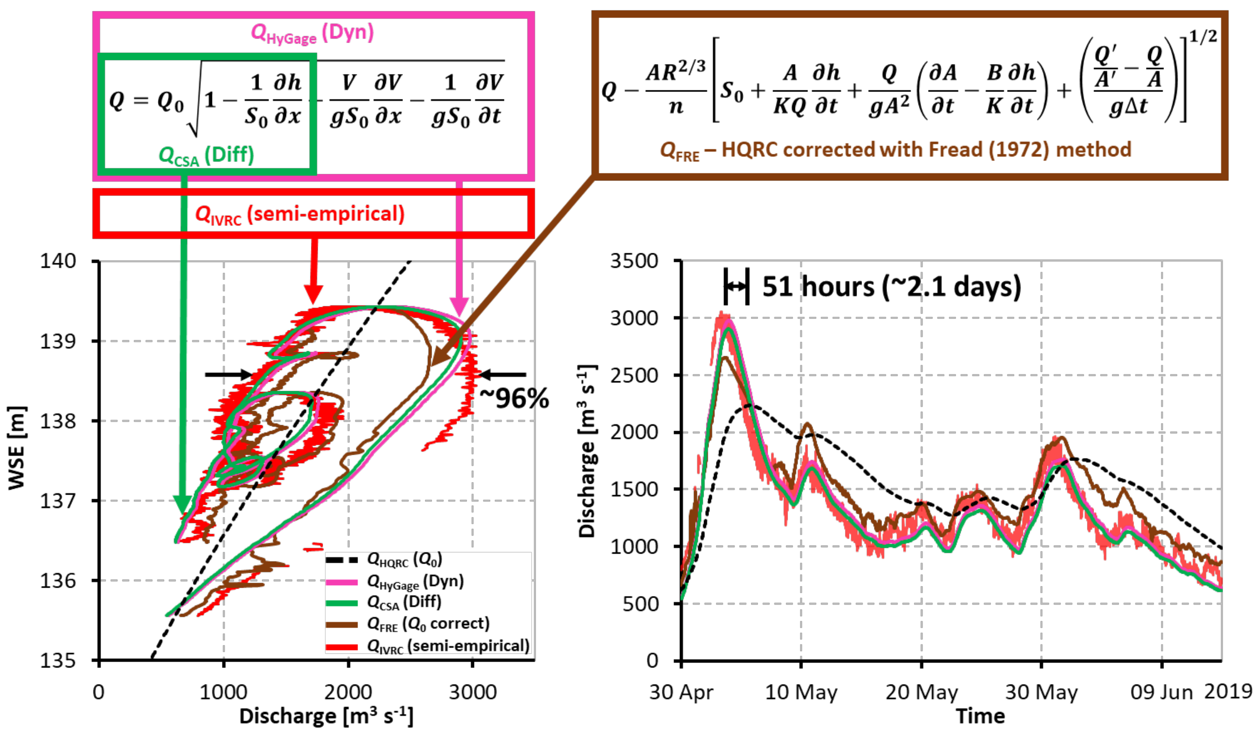

Figure 3. Comparison of the tracing of hysteretic features provided by various streamflow monitoring approaches.

HyGage Implementation

Ensuing from the above section, the HyGage monitoring concept combines measurement elements pertaining to IVRC (i.e., cross-section area and an index velocity) and CSA (i.e., cross-sectional areas and *FSS*) methods. Specifically, the HyGage relies on experimental procedures that provide the mean flow velocity (via V_{index} acquired in a point, over a line or surface in the water body) and the free-surface slope (*FSS*). There is a myriad of instruments available for acquiring these variables in real time including in-situ submersed or close- and remote-sensing technologies (Tsubaki et al., 2025). In this paper, we present the first published account of implementing the HyGage method at a full-scale, operational gaging station

For the Oxford HyGage test site, we deployed a horizontal Acoustic-Doppler Current Profiler (HADCP) and two Vertical ADCPs (VADCP) as schematically illustrated in Figure 4. The HADCP measures velocities across a line in the channel, while VADCPs measure velocities in verticals centered on the instruments. The free-surface elevations were measured with pressure sensors embedded in the ADCP units and with an independent bubbler in the central section of the test reach. The Oxford site has been intentionally over-instrumented to enable various redundant measurements for supporting the testing and validation of the HyGage protocols targeted through Muste et al. (2023) study. Notable, two HADCPs deployed in Sections 1 and 3 suffice to ensure that the hydraulic variable and their gradients are readily available for HyGage implementation.

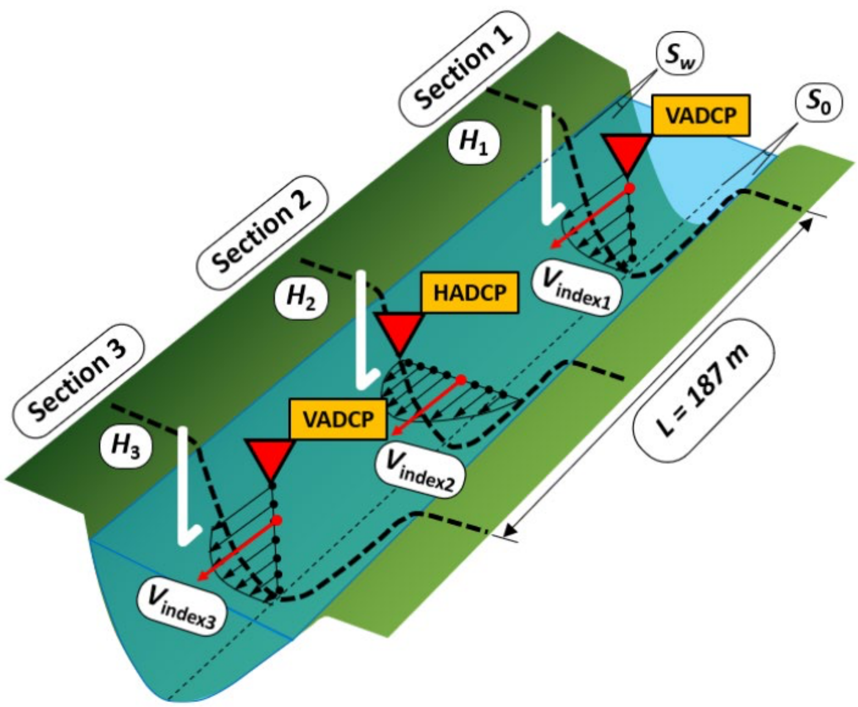

Figure 4. HyGage instrument layout at Oxford test site

EXPERIMENTAL RESULTS

Test sites

Essential specifications for the Grenoble-Campus and Oxford test sites are shown in Tab. 1. The selection of these sites followed a careful evaluation of their ability to satisfactorily meet the constraints inherent in the Saint-Venant equations. In particular, both gaging locations exhibit quasi-prismatic and relatively straight channel geometry in the vicinity of the station, a cross-section that remains stable over time, well-defined channel control at the measurement site, and minimal to no backwater influence. These characteristics collectively ensure that the underlying hydraulic assumptions of the governing equations are reasonably satisfied, thereby supporting reliable application of the monitoring methods under investigation. Prior studies revealed the stability and repeatability of the measurements with various methods applied to the two sites (Rousseau & Barthelemy, 2025 for Grenoble-Campus site and Lee et al., 2017 for Oxford site).

Table 1. Hydraulic specifications for the test stations analyzed in this study

Site (River)	Grenoble – Campus (Isère River)	Oxford (Clear Creek)
Site map		
Station equipment	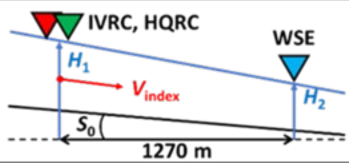	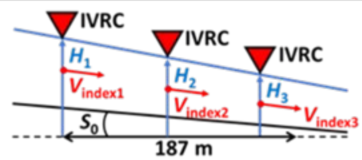
S_0	0.0004	0.00039
Base n	0.03	0.025
B [m]	68	10
B/h	27	15
$Q_{min-max}$ [m^3 s^{-1}]	≈ 43 – 1045	≈ 0.1 - 6
$Q_{annual\ mean}$ [m^3 s^{-1}]	175	0.7
Fr	0.19 – 0.30	0.16 – 0.24
Drainage area [km^2]	5570 (70% at altitude > 1000 m)	151

Grenoble-Campus Site Dataset

The datasets available at the Grenoble-Campus station are almost fully compliant with HyGage needs, missing only the convective acceleration term in Eq. (1). The purpose of including the Grenoble-Campus datasets in the analysis is two-fold. First, it demonstrates the performance of the CSA and IVRC methods working independently in capturing hysteretic features of interest. Secondly, it substantiates the CSA and IVRC contribution to the newly developed HyGage protocol that essentially is a hybrid of the two methods. The Grenoble-Campus site has been permanently equipped with a HQRC station since 1992 and is temporarily complemented by a variety of additional instruments deployed for hydrometric research and training conducted by the Institute of Environmental Geosciences (IGE), Electricity of France (EDF-DTG) and the National Research Institute for Agriculture, Food and the Environment (INRAE). Among the deployments, an IVRC station was operated for a short period. Taking advantage of the Isère - PDT stage gage installed in 2019 and located 1,270 m upstream from Grenoble-Campus, the CSA method is applied using the FSS measured between the two stations (see Tab. 1).

The flows at Grenoble-Campus station are controlled by a hydropower plant located 36.5 Km upstream at Le Cheylas and slightly influenced by a downstream dam at St. Egrève. Daily flow fluctuations are produced by turning on-off the hydropower turbines to accommodate grid energy needs. The sub-daily flow fluctuations are visualized by small-amplitude changes of the time series in Figure 5a. Discharge time series under 500 m^3s^{-1} (*WSE* = 211.86 m) at the Grenoble-Campus site reveal frequent flow pulses associated with the daily changes in the number of turbines operating at the upstream dam. The flow transitions produced by opening and closing the turbines under the 500 m^3s^{-1} discharge threshold trigger ST-GVFs of low magnitude. We include them in in the present analysis, despite that they are developing only weak hysteresis. The flows above 750 m^3s^{-1} are akin to a naturally controlled channel flow when the effect of the hydropower dam operations is not apparent at the gaging station.

The datasets analyzed at Grenoble-Campus for testing HyGage components are limited to only a short time interval because the instrumentation at this site is frequently changed to accommodate the needs for various hydrometric benchmarking and validation tests conducted at this experimental station. Through screening of the data in last five years, we found the April 1, 2021-December 31, 2022 time window to contain the most relevant input for testing the HyGage components (see Fig. 5a). The maximum flow in the last 30 years was recorded on November 15, 2023 (H= 6.71m, Q = 1047 m^3s^{-1}). This extreme event was still confined within the Isère River banks because of the levees constructed for protecting the area against floods. Given the extraordinary magnitude of the November 15, 2023, storm, we include it in the analysis despite that the IVRC datasets are not available.

The Isère gaging sites comprise the following instruments: Isère -PDT station (one OTT RLS radar level sensor - www.ott.com), Grenoble-Campus [one OTT PLS and one OTT PLS-C pressure level sensors and a temporarily deployed Horizontal Acoustic Doppler Current Profiler (ADCP) for index-velocity (Sontek-SL 1500 - www.xylem.com). The stage sensors of the two stations are connected to two Campbell Scientific CR1000 dataloggers (www.campbellsci.com). Instruments were sampled at different rates with synchronized timing (Thollet et al., 2021; Marggraf, 2024). Because the downstream stages are recorded at 30 minutes, the analysis is made with this time step. Illustrated in Figure 5b is the station's cross section along with the maximum stages for the two events selected for analysis. Figure 5c plots the HQRC rating used at the Grenoble-Campus station along with the traces of the flow for November 15, 2023, event determined with the Fread correction method, Q_{FRE}, applied to the operational HQRC. A cursory review of the flow traces indicates that, while they are different from the HQRC rating, their departure from the rating is small on both the rising and falling limbs of the hydrograph, indicating a mildly hysteretic site as subsequently discussed.

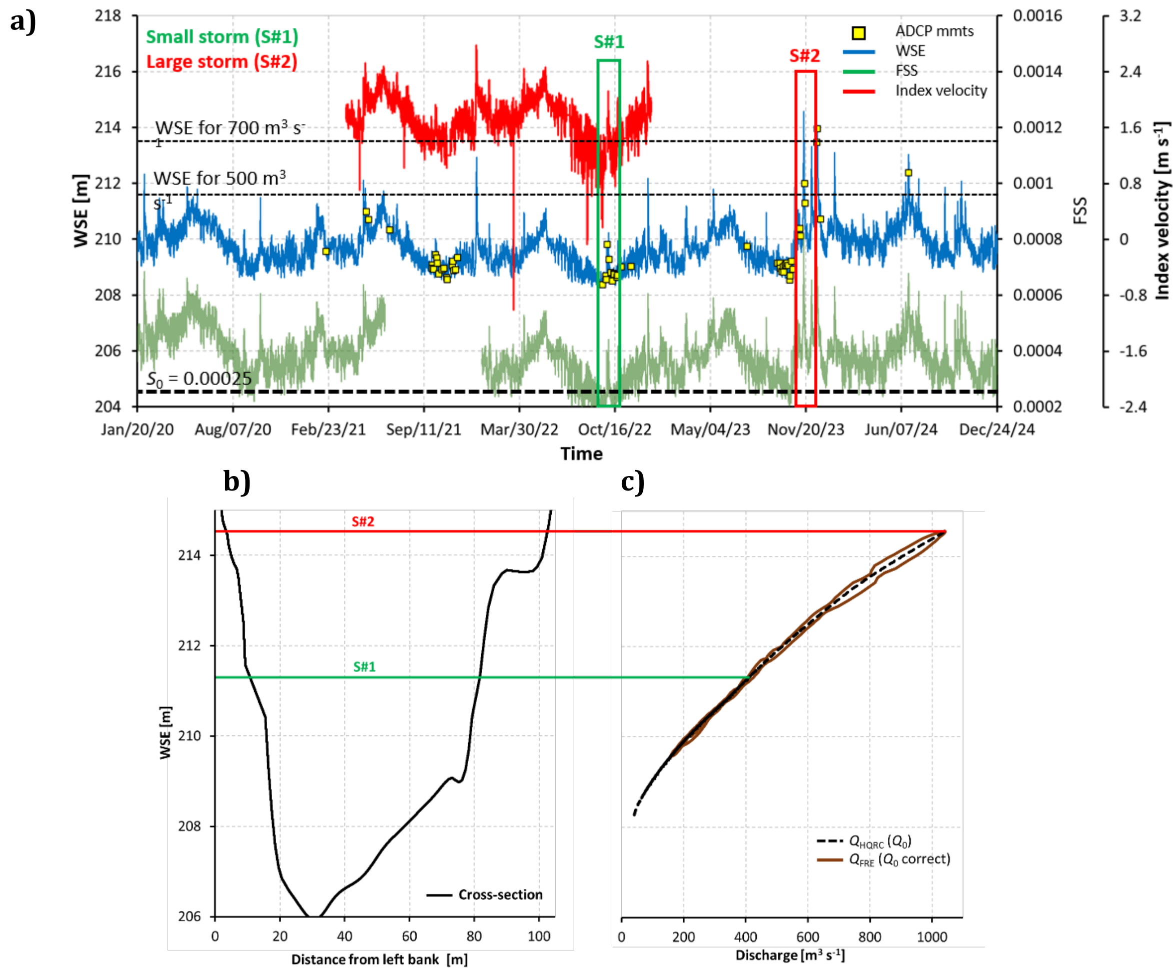

Figure 5. Analysis considerations for the Grenoble-Campus station: a) time series for the analyzed hydraulic variables; b) cross-section along with traces of the maximum stages for the two analyzed storm events; and c) the HQRC rating for the station (Q_0) along with the stage-discharge relationship estimated by Q_{FRE} correction method for the largest event.

Oxford Site Dataset

Given that the Oxford station was instrumented with the HyGage method testing in mind, the site comprises direct measurements of all the hydraulic variables and gradients appearing in Eq. (1) acquired with the best deployment and sampling practices. The maximum stage for the events propagating through the station at this station during 2020 – 2024 was reached at 215.4 m. The return period for the two events selected for analysis (S#1 and S#2 in Figure 6a) is less than 15 years, highlighting the prolonged drought at the experimental site during 2024 when the site was instrumented for tests. The stages for both events are below bankful elevation. Figure 6c illustrates the rating curve developed for this site using the Fenton (2018) method ($Q_{0\text{-}FEN}$) applied to all the direct measurements available at the station and the trace of the larger event reconstructed Fread method (Q_{FRE}).

The Oxford site is closely located with an HQRC operational station (USGS #05454220) installed 214 m upstream from the center of the HyGage test section (see Tab. 1). During the 2024 deployments, the station was equipped with two Vertical ADCPs (Sontek-IQ Plus) and a horizontal ADCP (Sontek-SL 1500), as illustrated in Figure 4. The VADCPs were located at the end of the test section and the HADCP was installed in the central cross section. The station's instruments were synchronized on the data logger clock to acquire data every 10 minutes. For this analysis, we used a 15-min step synchronized with the timing of the USGS data collection system. The flows at Oxford site and in the drainage area leading to the station are free of man-made hydraulic structures. It is worth noting that the flow traces for the two storms shown in Figure 6c do not exhibit readily visible hysteretic behavior. However, when the same events are examined using magnified axes in the subsequent analysis, the expected hysteresis patterns become unmistakably apparent, despite the relatively small magnitude of the 2024 storm events.

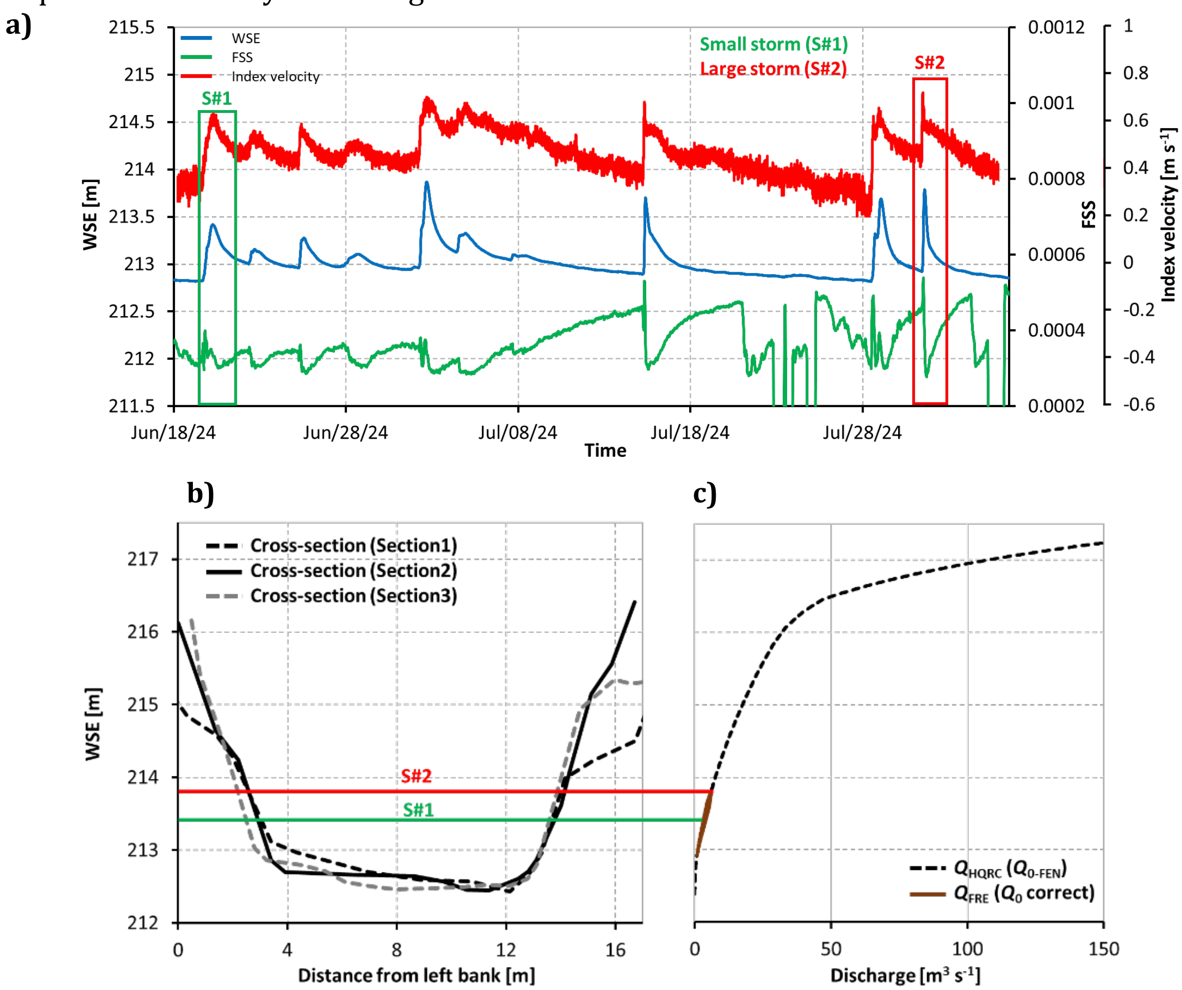

Figure 6. Analysis considerations for the Oxford station: a) time series for the analyzed hydraulic variables; b) cross-section along with traces of the maximum stages for the two analyzed storm events; and c) the reference HQRC for the site ($Q_{0\text{-}FEN}$) and the trace of the largest storms estimated with Fread method (Q_{FRE}).

Data Analysis at the Grenoble-Campus Site

Results are herein analyzed for S#1 and S#2 recorded at this station (see Fig. 5a). Given that the convective and local acceleration terms of the equation were not available for this site, the HyGage method cannot be applied in full. Figure 7 shows time-dependent and time-independent relationships among the primitive variables in Eq.1 (i.e., *WSE*, V_{index}, and *FSS*) measured at the station for the two storms selected for analysis.

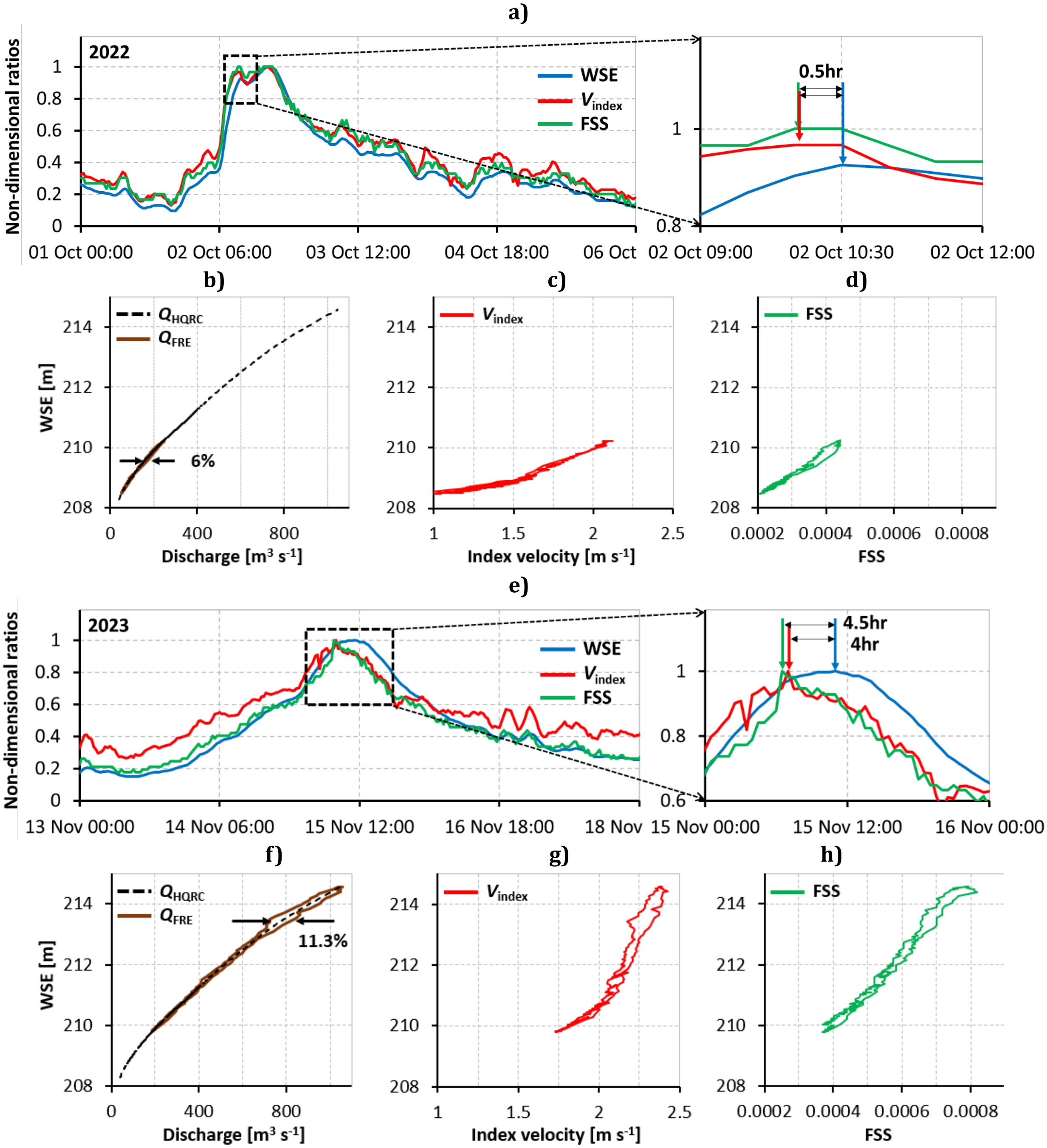

Figure 7. Hysteretic relationships for variables measured at Grenoble-Campus for storms S#1, S#2: a) time series for S#1; b), c), d) loops among variables for S#1; e) time series for S#2; f), g), h) loops among variables for S#2.

The time-dependent plots in Figs. 7a and 7c are represented in non-dimensional coordinates (normalization with the maximum value for the event) to offer a slightly different perspective on the hysteretic relationships between the hydraulic variables. Inspection of the plots in Figure 7 reveals that both storm events propagating through the station display hysteretic features that amplify with the magnitude of the flood waves. The frequent flow fluctuations produced at the hydropower upstream the Grenoble-Campus station are also evident especially at lower flows (see the tail of the hydrographs in Fig.7a).It is apparent that the hysteretic features at this site are relatively weak even for storm S#2, the largest one recorded at this site. The 11.3% loop size and 4.5hrs delay between the first and last hydrograph peaks for storm S#2 are just fractions of loop and lag magnitude shown in Fig.1 for Henry site, the most severe hysteretic site analyzed by the authors in prior analyses (House et al., 2025a; Muste et al, 2025a).

Oxford Site

Results are herein analyzed for S#1 and S#2 recorded at this station during the 2024 field campaign (see Fig. 6a). The primitive variables acquired to implement the full-fledged HyGage methodology at this site are shown in Fig. 8. Despite the small size of the river (i.e., a wadable stream), familiar hysteretic signatures are apparent in the data traces of 2024 storms #1 and #2. It is worth mentioning that this site was repeatedly tested over the years yielding ranges for the loop sizes and lags between variable peaks consistent with those captured during the 2024 storms (e.g., Lee et al., 2017; Muste et al., 2019).

The raw values for the variables and the spatiotemporal gradients necessary for HyGage implementation were acquired as follows (see also Fig. 4 for instrumentation arrangement): V_{index} was measured with the HADCP located in the center of the test reach; *FSS* time series were determined using the stages recorded by the pressure sensors embedded in the two VADCP located 187-m apart in the terminal sections of the test reach Sections 1 and 3 (see Figure 4). Stream stages (*WSE*) were measured with the pressure sensor located in the HADCP unit. An additional independent pressure sensor collocated with the HADCP was used for backing up data in equipment failure situations.

The conversion of V_{index} to V_{mean} required in Eq. 1 is accomplished with the entropy model described in the IVRC implementation section. The model uses as input HADCP velocities, and the cross section surveyed at the probe location. The model calibration and validation are executed with VADCP data collected in the same test reach. The choice for selecting the input and calibration/validation data could have been reversed but we preferred the first alternative as the HADCP was positioned at a low elevation where the velocity variation across the channel was relatively small. Velocities sampled in verticals by VADCPs enabled a more reliable verification of the entropy model. The discharges obtained with entropy model are labeled as $Q_{Entropy}$ in Figs. 9a and 9b. The Q_{IVRC} discharges in the same figures were obtained with the conventional index-velocity approach by pairing HADCP 15-min data with discharges estimated with the Q_{FRE} method. The $Q_{Entropy}$ vs. Q_{IVRC} comparison for the storm #2 (the largest of the 2024 field campaign) shows a good agreement between the two IVRC alternatives.

Figures 9c to 9f show discharges obtained with various monitoring methods along with stages in time-dependent and time-independent coordinates for the same storm. The simple HQRC rating for the test reach was determined using the station periodic measurements collected with Acoustic Doppler Velocimeter by USGS via the polynomial regression method of Fenton (2025). The plots in these figures include Q_{FRE} that aims to recover the dynamic part of the flow by analytically modifying the HQRC with the terms describing the propagation of a fully dynamic fluvial wave through the station.

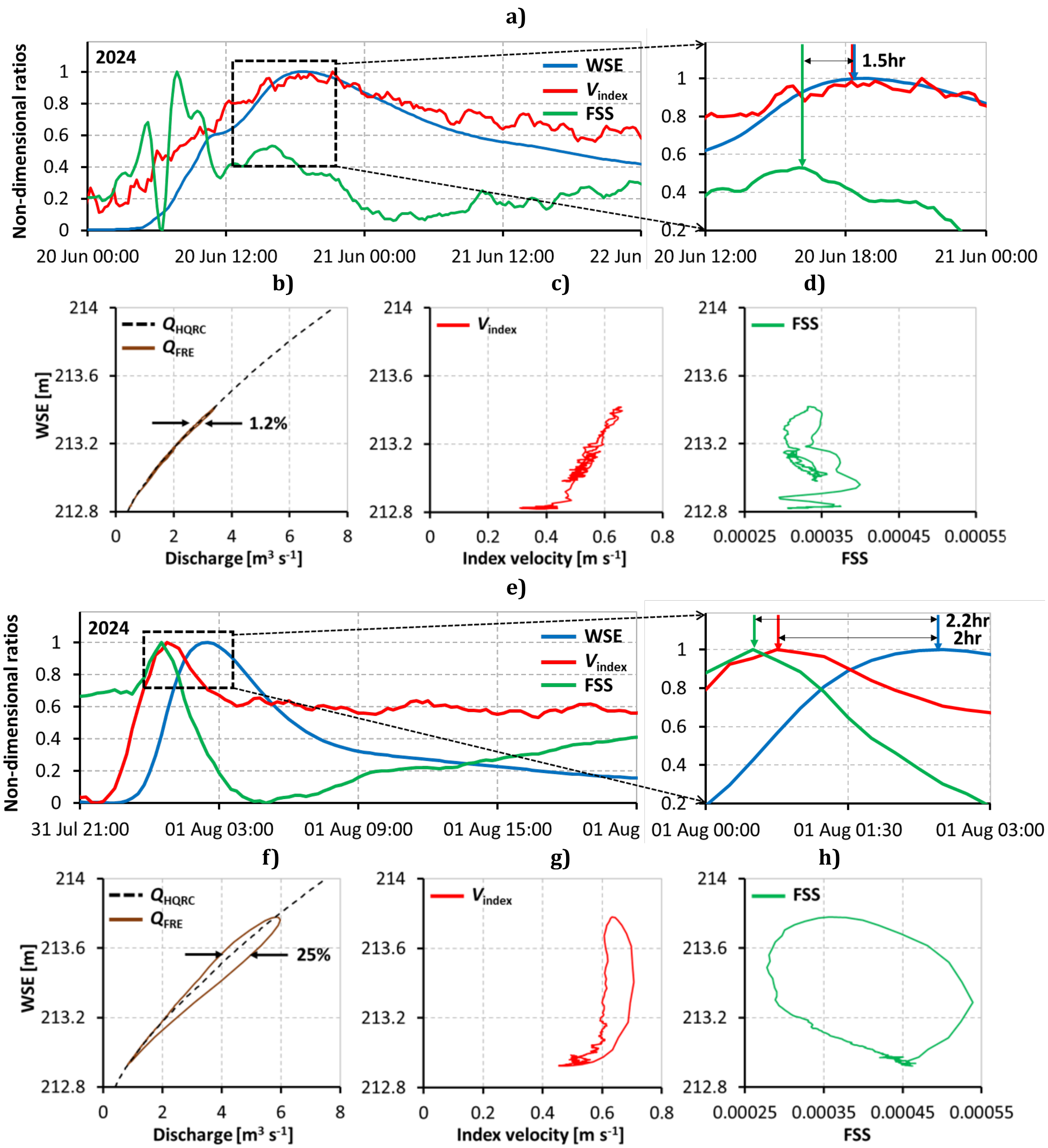

Figure 8. Hysteretic relationships for variables measured at Oxford for storms S#1 and S#2: a) time series for S#1; b), c), d) loops among variables for S#1; e) time series for S#2; f), g), h) loops among variables for S#2.

Figures 9c and 9d compare the discharges determined with the CSA method that demonstrated their efficiency in replicating actual unsteady flows due to the addition of the FSS to the stage measurements (Smith et al., 2010; Muste et al., 2019). Figures 9e and 9f highlight the performance of the HyGage method compared with the Q_{FRE} surrogate for tracing the actual flow for the 2024 storm #2. The series of plots illustrated in Figure 9 demonstrate the failure of the simple HQRC method to track unsteady flows contrasting unequivocally with the datasets delivered by the conventional IVRC and CSA methods as well as by those offered by the HyGage method.

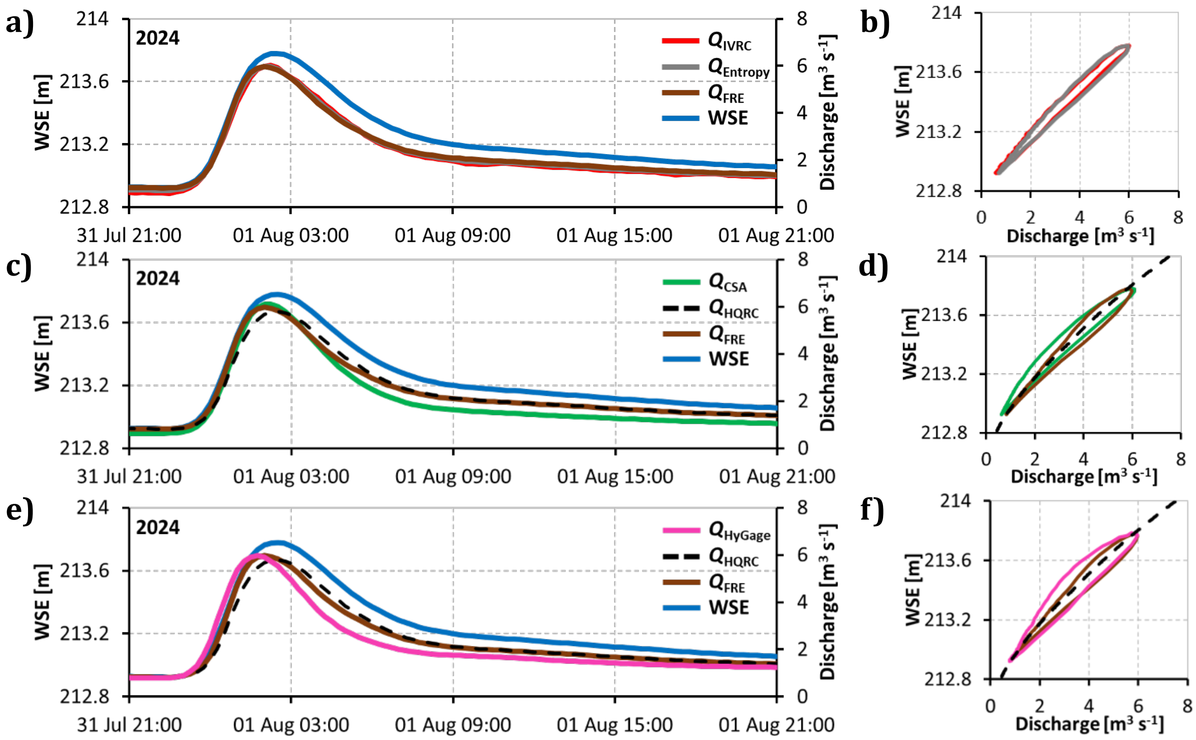

Figure 9. HyGage implementation at Oxford test site: a), b) validation of the entropy model for IVRC implementation; c), d) conventional "dynamic" monitoring approaches for discharge determination; e), f) HyGage performance in tracing actual unsteady flows

DISCUSSION

The analyses presented in the previous section show that the test sites examined in this study exhibit relatively weak hysteresis. It should be noted that these sites were selected for the availability of key data needed to evaluate HyGage capabilities, rather than for the severity of hysteresis during ST-GVFs. Additionally, the periods with usable data for testing HyGage components at Grenoble-Campus site and the full-fledged HyGage at Oxford site did not include GVF events suitable for assessing sensitivity to hysteresis magnitude. Neither site has independent, direct discharge measurements collected during ST-GVFs, which limits the availability of ground truth for evaluating the methods tested here. Such benchmark datasets with adequate temporal resolution are rarely available (e.g., Faye & Cherry, 1980) due to the high logistical and financial demands involved.

Despite these logistical limitations, the time-dependent and time-independent relationships among the primary hydraulic variables—water-surface elevation (*WSE*), index velocity (V_{index}), and free-surface slope (*FSS*)—displayed in Figures 7 and 8 show the expected hysteresis signatures. In particular, the link between hydrograph peak separation and the extent of the looped variable relationships, clearly reflect hysteretic behavior, even if the ST-GVFs are comparatively mild.

Another notable feature of the multi-variable relationships in Figure 7 and 8 is that the IVRC, CSA, and HyGage monitoring methods depart from the simple HQRC one-to-one relationship during the event propagation demonstrating that these methods recover the dynamic flow features missed by HQRC. Furthermore, it is also apparent that the sensitivity of the *FSS* loops is stronger compared with the stage vs. discharge and stage vs. index-velocity ones. This finding implies that hysteresis primarily affects the *WSE*–*FSS* relationship, underscoring the need to include this hydraulic variable when monitoring hysteresis-prone sites. The above-mentioned features have been apparent in prior studies conducted by the authors at multiple gaging sites (Muste et al. 2025a, 2025b).

The datasets analyzed herein substantiate some useful practical aspects of the HyGage implementation. The first considerations are referring to the conventional IVRC method that is the most mature monitoring method besides HQRC (at least in the US). A subject of clarification for future studies is the reliability and validity of the index-velocities measured with HADCPs that acquire velocities along a path length that is often a fraction of the river width, even for low stages. In this regard, Hoitink (2018), states that the side-installed HADCP should reach beyond the distance from the riverbank where the depth-averaged velocity exceeds the cross-section averaged velocity, a requirement quite difficult to achieve in rivers with pronounced cross-section variability. Moreover, the physical relevance of sampling velocity profiles along horizontal lines of sight is questionable in comparison with sampling vertical velocity distributions in the deep portion of the cross section. Problems such as temporary changes in the flow field structure due to secondary currents can be more detrimental in reconstructing the 2-D cross-sectional velocity distribution from limited horizontal sampling compared with the measurement acquiring of the velocity profile in one relevant vertical and extrapolating this distribution profile over the river width (Le Coz et al., 2008). Finally, the persistence of the HADCP failure to measure velocity in the far-field area of the acoustic path requires first to identify the source of the problem (e.g., loss in the signal return) and subsequently finding robust corrections that require a limited number of additional in-situ verification measurements.

An additional consideration regarding the IVRC method is the proven efficiency of the entropy model to replace the laborious IVRC method. For the present study, index-velocities (V_{index}) were acquired along a horizontal path and converted to cross-sectional velocity (V_{mean}) distribution using a relatively small number of input data and physical governing laws. The advantages of the entropy model entail flexibility in adopting various instruments for the index-velocity measurements (i.e., in singular points, over a vertical or horizontal line of sight or over surfaces in the body of water) and attaining a computational speed that can be implemented in real time. An additional benefit of the entropy model is enabling to compute the stream discharge (Q) using analytical means rather than making recourse to empirical correlations between in-situ measured variables (V_{index} and Q) supported by statistical analyses that do not always account for the actual flow mechanisms. Recent studies suggest that the entropy model is increasingly used as an alternative for conventional IVRC method implemented various index-velocity measurement approaches (e.g., Moramarco et al., 2019; Bahmanpouri et a., 2022; Kechnit et al., 2024; Singh, 2025).

Other useful practical considerations can be drawn regarding the implementation of the CSA method, a viable monitoring approach increasingly used for monitoring ST-GVFs. A closer inspection of the *FSS* time series trends illustrated in Figs. 8a, 8e vs. those in Figs. 9a, 9e substantiate that in the former case the *FSS* hydrograph does not display a depression following its peak, while in the latter case a *FSS* dip is visible for both storm time series. This difference in *FSS* pattern is most probably related to a longer than optimal distance between the location of stage sensors as demonstrated with numerical simulations in House et al. (2025a). Currently, efforts to obtain *FSS* over large scales using remote sensing are increasingly tackled using satellite-borne instrumentation (Sichangi, et al., 2018; Bauer-Gottwein et al., 2024; Dhote et al., 2025; Wang et al., 2025).

Along with previously analyses of more than 20 gaging sites worldwide (Muste et al., 2022b; 2025b), this study confirms deviations of actual flows from those estimated with the routinely used HQRC even if the sites are affected by weak hysteresis. Specifically, the present study confirms that hysteresis is site- and event-dependent as indicated by the 1.6% to 96% range for the four storms analyzed herein (see Figs. 7b, 7f, 8b and 8f). These departures can be seen as uncertainty intervals in the data provided by HQRC. Most of the differences are considerably larger than the customarily 5% tacitly accepted in practice (Schmidt, 2002). At the present time, there is scarce evidence of the impact of the three leading causes to produce hysteresis (i.e., the local slope of the channel bed, the flashiness and the magnitude of the Fr numbers of the propagating waves) acting alone or in different combinations. Scant and frugal analytical inferences, not fully vetted with experimental evidence, are broadly hinting that value of the bed slope is a dominant causal factor. For example, Dottori et al. (2009) indicate that rivers with bed slopes (S_0) smaller than 5×10^{-4} are potentially displaying hysteresis while Fread (1975) propose 1×10^{-4} for the same criterion. Perumal et al. (2006) suggest the $|(1/S_0)\,\partial h\,/\,\partial x| \leq\ 0.5)$ criterion to distinguish between kinematic and diffusive waves, hence the presence or absence of hysteresis in HQRCs due to unsteady flows. More of these types of diagnostic formulas need to be tested to assess hysteresis presence and its severity to inform on the necessity for alternative monitoring flow protocols at new or existing monitoring sites.

Given that the implementation and operation of the methods for continuous in situ streamflow monitoring come with sizable expenses, the decision whether a dynamic rating curve is needed for a specific combination of factors should be based on a rigorous assessment of the site morphological and hydrological characteristics and faithful cost-benefit analyses, as described in Muste et al. (2025b). Table 2 lists rough cost estimates associated with IVRC, CSA, and HyGage implementation (USGS 2024, personal communication). The actual costs for a specific situation are highly variable depending on the monitoring infrastructure existent at the site (i.e., old or new gage), the instrument accuracy and the role of the gaging station (i.e., monitoring, flood hazard forecasting).

Table 2. Comparative analysis of the costs for various types of monitoring approaches*

Method	HQRC	IVRC	CSA	HyGage
Cost referenced to HQRC (%)	reference	+15	+26	+43

*Cost estimations include operation and maintenance and are instrument- and method-dependent

In addition to improving the time series accuracy in ST-GVF monitoring and maintaining its efficiency in monitoring steady flows, the HyGage measurement capabilities offer promising opportunities for further enhancing hydrologic monitoring and modeling and fundamental investigations of these complex flows. Previous works identified features of the data provided by the dynamic rating methods that are not fully investigated yet (Perumal et al., 2006; Dottori et al., 2009). Table 3 lists hydrological/hydraulic hydrometric issues that are facilitated by HyGage data usage toward the benefit of various aspects of river multi-task monitoring, modeling, and forecasting.

Table 3. Features of the HyGage measured data that broaden their significance and usage

#	HyGage data features	HyGage data significance & usage
1	Use of Eq. (1) as base for HyGage method accounts for gradual variation of the flow stage in space and time	The method captures accurately discharges during unsteady and backwater flows as well as in various combinations of these flow regimes
2	Use of an analytical relationship between measured variables and their gradients	Elimination of empirical adjustment factors and of statistical tools that are not always physically justifiable. The streamflow monitoring equations are akin to those used in numerical modeling of ST-GVFs.
3	Precise estimation of the peak discharge magnitude and timing (missed by HQRC)	Improvement of data accuracy for calibration/validation of rainfall-runoff and flood routing models and for their assimilation in streamflow forecasting models
4	Precise indication of the magnitude and arrival time for the flood crest	Re-evaluation of the methodology for estimation of peak flow, flow volumes and loads of transported matter (particulate and in suspension) during ST-GVFs
5	Continuous data over the whole duration of ST-GVFs	Reducing the errors introduced by extrapolation of the HQRC ratings at higher flow regimes
6	Capturing the phasing of the peak variable hydrographs	The inherent hydrograph succession (i.e., FSS, velocity, stage) in ST-GVFs can be used to flag the subsequent occurrence of the flood crest timing
7	Inclusion of the directly measured derivative $\partial h / \partial x$	The measured derivative $\partial h / \partial x$ enables calculation of $\partial^2 h/\partial x^2$ during a ST-GVF event. The inflexion points in the representation of $\partial^2 h/\partial x^2$ are related to critical control points in the progression of the primitive variable hydrographs.
8	Inclusion of directly measured $\partial V / \partial x$ and $\partial V / \partial t$ gradients	The rate changes are direct reflection of reach- or local spatial changes occurring at the station. Their presence can warn that additional site inspections are needed to verify the validity of the initial gaging site conditions.

A promising line of developments for advancing HyGage implementation is offered by recent attempts to quantify hydraulic variables in large rivers with remote sensing observations acquired from satellites that do not require in-situ infrastructure. Such examples are the measurement of river water surface elevation, width, and slope over river reaches targeted by the Surface Water and Ocean Topography Mission (Andreadis et al.,

2025) and the emerging effort to evaluate free-surface velocity using the Fluvial Video from Satellite – FluViSat (https://www.ceh.ac.uk/our-science/projects/Fluvisat). The continuous exploration of new hydrometric techniques opens opportunities for equipping HyGage with more cost-efficient instrument arrangements while also expanding the coverage area from gaging at one point to simultaneous gaging at multiple sites within watershed with minimal addition for the infrastructure cost.

CONCLUSION

The HyGage monitoring method described in this study belongs to the family of dynamic discharge estimation approaches examined through numerical simulations by Dottori et al. (2009) and applied in situ through the semi empirical protocols of the index velocity method (Levesque & Oberg, 2012) and the continuous slope area method (Smith et al., 2010). These approaches have gained prominence among monitoring agencies, particularly at sites where hysteresis poses challenges to conventional stage–discharge techniques. HyGage advances this approach by integrating components of both methods within a unified, physically based framework and by eliminating the dependence on semi empirical rating curves. A further improvement for HyGage implementation is the incorporation of the entropy-based conversion of the index velocity to mean cross sectional velocity with minimum data input.

The comparative analysis presented in this paper—featuring the index velocity method, the continuous slope area method, and the rating independent HyGage formulation—demonstrates the ability of these approaches to capture hysteretic behavior characteristic of spatiotemporal gradually varied flow. These features, routinely overlooked by the widely used height–discharge rating curve method, are resolved by HyGage without sacrificing applicability under steady flow conditions. Indeed, when the gradients in Eq. (1) become negligible, the HyGage discharge formulation converges to the conventional stage–discharge relationship, which has been extensively validated for such regimes.

Although the primary objective of this paper is to evaluate the capacity of HyGage to accurately characterize gradually varied flows, the departures between HyGage derived discharges and those obtained from traditional stage–discharge relations remain modest at the analyzed sites due to their mildly hysteretic nature. Nonetheless, the presence of distinct hysteretic patterns across both rising and falling hydrograph limbs underscores the value of HyGage for capturing the full dynamics of fluvial wave propagation. The HyGage capability to distinguish subtle flow mechanisms in ST-GVFs is essential for improving the efficiency, reliability, and operational utility of hydrometric data, thereby enabling enhanced situational awareness, more accurate streamflow forecasting, and more informed decision making across a broad range of riverine environments.

Recent advances in sensing technologies—many capable of measuring stage, index velocity, and free surface slope within a single instrument and deployable across submerged, close range, and remote sensing platforms—position HyGage as a highly adaptable framework for quantifying the primitive variables necessary for discharge estimation in real time.

Given the HyGage operational flexibility and the hydrometric community's growing shift toward dynamic, physics-based methods, future studies are expected to build on the analytical framework presented here to ensure robust operational deployment of HyGage that aligns with contemporary scientific standards and continuing to expand its capabilities to new fit-for-purpose applications.

Acknowledgements

This work was supported by the National Science Foundation (NSF-EAR-HS 2139649) and by the National Oceanic and Atmospheric Administration (NOAA) through the Cooperative Institute for Research on Hydrology (CIROH), under the NOAA Cooperative Agreement with The University of Alabama (NA22NWS4320003). We are grateful for the steady and invaluable support for setting instrumentation at the Oxford site provided by our colleagues: Loeser T., Everhart R., Lamoreaux, A., Barquist B. (IIHR-Hydroscience & Engineering), and Lynch M. (Xylem/Sontek).

References

Andreadis, K. M., Coss, S. P., Durand, M., Gleason, C. J., Simmons, T. T., Tebaldi, N., et al., 2025. A first look at river discharge estimation from SWOT satellite observations. *Geophysical Research Letters* 52, e2024GL114185. https://doi.org/10.1029/2024GL114185

Aricò, C., Nasello, C., Tucciarelli, T., 2009. Using unsteady-state water level data to estimate channel roughness and discharge hydrograph. *Advances in Water Resources* 32(8), 1223–1240. https://doi.org/10.1016/j.advwatres.2009.05.001

Bahmanpouri, F., Barbetta, S., Gualtieri, C., Ianniruberto, M., Filizola, N., Termini, D., Moramarco, T., 2022. Prediction of river discharges at confluences based on entropy theory and surface velocity measurements. *Journal of Hydrology*.

Bauer-Gottwein, P., Christoffersen, L., Musaeus, A., Frías, M. C., Nielsen, K., 2024. Hydraulics of time-variable water surface slope in rivers observed by satellite altimetry. *Remote Sensing* 16, 4010. https://doi.org/10.3390/rs16214010

Beven, K., 2006. Searching for the Holy Grail of scientific hydrology: Qt = (S, R, Δt)A as closure. *Hydrology and Earth System Sciences* 10, 609–618. https://doi.org/10.5194/hess-10-609-2006.

Beven, K. 2016. Facets of uncertainty: epistemic uncertainty, nonstationarity, likelihood, hypothesis testing, and communication, Hydrological Sciences Journal, 61:9, 1652-1665, doi: 10.1080/02626667.2015.1031761

Boyer, M. C., 1937. Analysis of methods of adjusting stage and discharge for measurements during changing stage. Unpublished manuscript, Water-Resources Branch, U.S. Geological Survey, 192–200.

Chiu, C.-L., 1988. Entropy and 2-D velocity distribution in open channels. *Journal of Hydraulic Engineering* 114(7), 738–756.

Chiu, C.-L., 1989. Velocity distribution in open channels. *Journal of Hydraulic Engineering* 115(5), 576–594. https://doi.org/10.1061/(ASCE)0733-9429(1989)

Chow, V. T., 1959. *Open-channel hydraulics*. McGraw-Hill Book Co., New York, NY.

Dalrymple, T., Benson, M. A., 1967. Measurement of peak discharge by the slope-area method. *U.S. Geological Survey Techniques of Water-Resources Investigations*, book 3, chap. A2, 12 pp.

Darienzo, M., Renard, B., Le Coz, J., Lang, M., 2021. Detection of stage-discharge rating shifts using gaugings: A recursive segmentation procedure accounting for observational and model uncertainties. *Water Resources Research* 57, e2020WR028607. https://doi.org/10.1029/2020WR028607

Dhote, P. R., Agarwal, A., Paris, A., Singhal, G., Thakur, P. K., Oubanas, H., et al., 2025. Unveiling the first impressions of the wide-swath altimetry SWOT mission over the Ganga River, India. *Geophysical Research Letters* 52, e2025GL115402. https://doi.org/10.1029/2025GL115402

Di Baldassarre, G., Montanari, A., 2009. Uncertainty in river discharge observations: A quantitative analysis. *Hydrology and Earth System Sciences* 13(6), 913–921. https://doi.org/10.5194/hess-13-913-2009

Dottori, F., Martina, L. V., Todini, E., 2009. A dynamic rating curve approach to indirect discharge measurements. *Hydrology and Earth System Sciences* 13, 847–863.

Dottori, F., et al., 2018. Increased human and economic losses from river flooding with anthropogenic warming. *Nature Climate Change* 8, 781–786.

Dykstra, S. L., Dzwonkowski, B., 2020. The propagation of fluvial flood waves through a backwater-estuarine environment. *Water Resources Research* 56, e2019WR025743. https://doi.org/10.1029/2019WR025743

Faye, R. E., Cherry, R. N., 1980. Channel and dynamic flow characteristics of the Chattahoochee River, Buford Dam to Georgia Highway 141. *U.S. Geological Survey Water-Supply Paper* 2063.

Fenton, J. D., 2001. in *Proceedings of the Conference on Hydraulics in Civil Engineering*, 28–30

Fenton, J. D., 2018. On the generation of stream rating curves. *Journal of Hydrology* 564, 748–757. https://doi.org/10.1016/j.jhydrol.2018.07.025

Fenton, J. D., 2025. Velocity distributions in open channels and the calculation of discharge. *Journal of Irrigation and Drainage Engineering* 151(2). https://orcid.org/0000-001-5045-5968

Ferrick, M. G., 1985. Analysis of river wave types. *Water Resources Research* 21(2), 209–220.

Fread, D. L., 1975. Computation of stage-discharge relationship affected by unsteady flow. *Water Resources Bulletin*, 11(2), 429–442.

Henderson, F. M., 1966. *Open channel flow*. Macmillan Company, New York, NY, 522 pp.

Herschy, R. W., 2009. *Streamflow measurement* (3rd ed.). CRC Press. https://doi.org/10.1201/9781482265880

Hoitink, A. J. F., 2018. Monitoring and analysis of lowland river discharge. In: *Proceedings of River Flow Conference* (IAHR), 5–8 September 2018, Lyon, France. https://doi.org/10.1051/e3sconf/20184006045

Holmes, R. R., 2016. River rating complexity. In: *Proceedings of River Flow Conference*. Taylor & Francis Group, St. Louis, MO, USA. ISBN 978-1-138-02913-2.

House, E., Kim, K., Muste, M., Meselhe, E., Demir, I., 2025a. Back to basics: On the proper determination of free-surface slope (FSS) in gradually varied open channel flows. *Flow Measurement and Instrumentation* 102979.

House, E., Meselhe, E., Muste, M., Demir, I., 2025b. Streamflow hysteresis analysis through a deep-dive budget of the St Venant equation momentum terms. *Water Resources Research* 61, e2024WR038103. https://doi.org/10.1029/2024WR038103

Hidayat, H., Vermeulen, B., Sassi, M. G., Torfs, P. J. J. F., Hoitink, A. J. F., 2011. Discharge estimation in a backwater affected meandering river. *Hydrology and Earth System Sciences* 15, 2717–2728. https://doi.org/10.5194/hess-15-2717-2011

Ikhouane, F., 2013. Characterization of hysteresis process. *Mathematics of Control, Signals, and Systems* 25, 291–310. https://doi.org/10.1007/s00498-012-0099-6

ISO, 1992. Liquid flow measurement in open channels – slope-area method, International Organization for Standardization, *ISO 1070:1992*, Geneva. http://www.iso.org/iso/catalogue_detail.htm?csnumber=5564

Johnson, E. D., Cowen, E. A., 2017. Remote determination of the velocity index and mean streamwise velocity profiles. *Water Resources Research* 53, 7521–7535. https://doi.org/10.1002/2017WR020504

Jones, B. E., 1915. A method of correcting river discharge for a changing stage. *U.S. Geological Survey Water-Supply Paper* 375-E, 117–130.

Julien, P., 2018. *River mechanics* (2nd ed.). Cambridge University Press, United Kingdom.

Kechnit, D., Tshimanga, R. M., Ammari, A., Trigg, M. A., Carr, A. B., Bahmanpouri, F., Moramarco, T., 2024. Bathymetry and discharge estimation in large and data-scarce rivers using an entropy-based approach. *Hydrological Sciences Journal* 69(15), 2109–2123.

Kennedy, E., 1984. Discharge ratings at gaging stations. *U.S. Geological Survey Techniques of Water-Resources Investigations*, book 3, chap. A10, 59 pp.

Kim, K., Muste, M., Hauet, A., 2025. Analytical estimation of cross-sectional velocity distribution using index-velocity acquired with horizontal Acoustic Doppler Current Profilers (H-ADCP). *AGU Fall Meeting*, 15–19 December 2025, New Orleans, LA.

Kreibich, H., et al., 2022. The challenge of unprecedented floods and droughts in risk management. *Nature*, 1–5.

Lee, K., Firoozfar, A.R., Muste, M., 2017. Monitoring of unsteady open channel flows using continuous slope-area method, *Hydrol. Earth Syst. Science*, 21 pp.1863-1874; doi:10.5194/hess-21-1863-2017.

Laenen, A., 1985. *Acoustic velocity meter systems*, USGS Techniques of Water-Resources Investigations, Book 3, Chapter 17.

Lamoreux, A., Kim, K., Williams, P., Muste, M., 2025. Monitoring the temporal variation of riparian vegetation roughness. *AGU Fall Meeting*, 15–19 December 2025, New Orleans, LA.

Le Coz, J., Pierrefeu, G., Paquier, A., 2008. Evaluation of river discharges monitored by a fixed side-looking Doppler profiler. *Water Resources Research* 44, 1–13.

Lee, K., Firoozfar, A. R., Muste, M., 2017. Monitoring of unsteady open channel flows using continuous slope-area method. *Hydrology and Earth System Sciences* 21, 1863–1874. https://doi.org/10.5194/hess-21-1863-2017

Levesque, V. A., Oberg, K. A., 2012. *Computing discharge using the index velocity method*. U.S. Department of the Interior, U.S. Geological Survey.

Litrico, X., Fromion, V., 2009. *Modeling and control of hydrosystems*. Springer, 409 pp. https://doi.org/10.1007/978-1-84882-624-3

Mansanarez, V., Renard, B., Le Coz, J., Lang, M., Darienzo, M., 2019. Shift happens! Adjusting stage-discharge rating curves to morphological changes at known times. *Water Resources Research* 55, 2876–2899. https://doi.org/10.1029/2018WR023389

Marggraf, J. 2024. Improving methods for the hydroacoustic monitoring of suspended sand concentration and grain size : application to the Isère River at Grenoble Campus, PhD Thesis, Université Claude Bernard - Lyon I, English.

McMillan, H., Seibert, J., Petersen-Overleir, A., Lang, M., White, P., Snelder, T., et al., 2017. How uncertainty analysis of streamflow data can reduce costs and promote robust decisions in water management applications. *Water Resources Research* 53, 5220–5228. https://doi.org/10.1002/2016WR020328

Moramarco, T., Saltalippi, C., Singh, V. P., 2004. Estimation of mean velocity in natural channel based on Chiu's velocity distribution equation. *Journal of Hydrologic Engineering* 9, 42–50. https://doi.org/10.1061/(ASCE)1084-0699(2004)9:1(42)

Moramarco, T., Pandolfo, C., Singh, V. P., 2008. Accuracy of kinematic wave and diffusion wave approximations for flood routing. I: Steady analysis. *Journal of Hydrologic Engineering* 13(11), 1078–1088.

Moramarco, T., Barbetta, S., Tarpanelli, A., 2017. From surface velocity measurements to discharge assessment by entropy theory. *Water* 9, 120. https://doi.org/10.3390/w9020120

Moramarco, T., Barbetta, S., Bjerklie, D. M., Fulton, J., Tarpanelli, A., 2019. River bathymetry estimate and discharge assessment from remote sensing. *Water Resources Research* 55, 6692–6711. https://doi.org/10.1029/2018WR024220

Moussa, R., Bocquillon, C., 1966. Criteria for the choice of flood-routing methods in natural channels. *Journal of Hydrology* 186, 1–30.

Muste, M., Bacotiu, C., Thomas, D., 2019. Evaluation of the slope-area method for continuous streamflow monitoring. In: *Proceedings of the 38th World Congress*, 1–6 September 2019, Panama City, Panama.

Muste, M., Lee, K., Kim, D., Bacotiu, C., Rojas Oliveros, M., Cheng, Z., Quintero, F., 2020. Revisiting hysteresis of flow variables in monitoring unsteady streamflows. *Journal of Hydraulic Research* 58(6), 867–887. https://doi.org/10.1080/00221686.2020.1786742

Muste, M., Kim, D., Kim, K., 2022a. A flood-crest forecast prototype for river floods using only in-stream measurements. *Communications Earth & Environment* 3(1), 78.

Muste, M., Kim, D., Kim, K., 2022b. Insights into flood wave propagation in natural streams as captured with acoustic profilers at an index-velocity gaging station. *Water* 14, 1380. https://doi.org/10.3390/w14091380

Muste, M., 2023. Novel physically-based streamflow monitoring methodology. CIROH Award: NA22NWS4320003, National Weather Service/National Oceanic and Atmospheric Administration.

Muste, M., Kim, K., Kim, D., Fleit, G., 2025a. Decoding the hysteretic behavior of hydraulic variables in lowland rivers with multivariate monitoring approaches. *Hydrological Processes*. https://doi.org/10.1002/hyp.70008

Muste, M., Kim, K., Kim, D., Demir, I., 2025b. Comparative analysis of the stage-discharge rating operated in gradual varied flows with alternative streamflow monitoring approaches. Preprint, *EarthArXiv*. https://doi.org/10.31223/X52Q7X

Nihei, Y., Kimizu, A., 2008. A new monitoring system for river discharge with horizontal acoustic Doppler current profiler measurements and river flow simulation. *Water Resources Research* 44, W00D20. https://doi.org/10.1029/2008WR006970

Perret, E., Lang, M., Le Coz, J., 2022. A framework for detecting stage-discharge hysteresis due to flow unsteadiness: Application to France’s national hydrometry network. *Journal of Hydrology* 608, 127567. https://doi.org/10.1016/j.jhydrol.2022.127567

Perumal, M., Shrestha, K. B., Chaube, U. C., 2006. Reproduction of hysteresis in rating curves. *Journal of Hydrologic Engineering* 130, 870–878.

Petersen-Øverleir, A., 2006. Modelling stage–discharge relationships affected by hysteresis using the Jones formula and nonlinear regression. *Hydrological Sciences Journal* 51(3), 365–388.

Prowse, C. W., 1984. Some thoughts on lag and hysteresis. *Area* 16(1), 17–23.

Rantz, S. E., et al., 1982. *Measurement and computation of streamflow*. U.S. Geological Survey Water-Supply Paper 2175, Vols. 1–2.

Rousseau, C., Barthelemy, É., 2025. Mesure de la pente hydraulique de l'Isère à Grenoble. *Recherche Data Gouv*, V1. https://doi.org/10.57745/OQ7I5F

Rozos, E., Leandro, J., Koutsoyiannis, D., 2022. Development of rating curves: Machine learning vs. statistical methods. *Hydrology* 9, 016. https://doi.org/10.3390/hydrology910016

Saint-Venant, A. J. C. Barré de, 1871. Théorie du mouvement non permanent des eaux, avec application aux crues des rivières et à l'introduction de marées dans leurs lits. *Comptes Rendus de l'Académie des Sciences* 73, 147–154 and 237–240.

Sauer, V. B., Turnipseed, D. P., 2010. Stage measurement at gaging stations. *U.S. Geological Survey Techniques and Methods*, book 3, chap. A7, 45 pp. http://pubs.usgs.gov/tm/tm3-a7

Schwatke, C., Halicki, M., Scherer, D., 2024. Generation of high-resolution water surface slopes from multi-mission satellite altimetry. *Water Resources Research* 60, e2023WR034907. doi.org/10.1029/2023WR034907

Schmidt, A. R., 2002. Analysis of stage-discharge relations for open-channel flows and their associated uncertainties. PhD dissertation, University of Illinois at Urbana–Champaign, Urbana, IL.

Schmidt, A. R., Garcia, M. H., 2003. Theoretical examination of historical shifts and adjustments to stage-discharge rating curves. In: *ASCE World Water & Environmental Resources Congress*, Philadelphia, PA.

Schmidt, A.R., Yen, B.C. 2009. Theoretical development of stage-discharge ratings for subcritical open-channel flows, Journal of Hydraulic Engineering, 134(9), doi: 10.1061/(ASCE}0733-9429(2008)134:9(1245)

Sermet, Y., Demir, I., 2023. Camera-based intelligent stream stage sensing for decentralized environmental monitoring. *Journal of Hydroinformatics* 25(2), 163–173.

Sichangi, A. W., Wang, L., Hu, Z., 2018. Estimation of river discharge solely from remote-sensing derived data: An initial study over the Yangtze River. *Remote Sensing* 10, 1385. https://doi.org/10.3390/rs10091385

Singh, V. P., 2025. Entropy in hydrology. *Perspectives of Earth and Space Scientists* 6, e2025CN000272. https://doi.org/10.1029/2025CN000272

Smith, C. F., Cordova, J. T., Wiele, S. M., 2010. The continuous slope-area method for computing event hydrographs. *U.S. Geological Survey Scientific Investigations Report* 2010–5241, 37 pp.

Thollet, F., Rousseau, C., Camenen, B., Boubkraoui, S., Branger, F., Lauters, F., Nemery, J., 2021. Long term high frequency sediment observatory in an alpine catchment: The Arc-Isère rivers, France. Hydrological Processes. 35, e14044, doi.org/10.1002/hyp.14044

Tsubaki, R., Moramarco, T., Manatis, G., Le Coz, J., Muste, M., 2025. Advances in river measurement technologies. Invited paper for *New Waves in Hydrometry (Japan)*, Vol. 1, 36–59.

USGS, 2010. Continuous records processing of all water time series data. Water Resources Discipline Policy Memorandum 2010.02. http://water.usgs.gov/admin/memo/policy/wrdpolicy10.02.html

USPTO (2026). Measurement system for streamflow determination in real time, University of Iowa Research Foundation, United States Patent and Trademark, Patent No. 12.529.586, January 20, 2026.

Wang, Y., Morton, Y. J., Minear, J. T., Putnam, A., Conrad, A., Axelrad, P., Nerem, R. S., Warnock, A., Ruf, C., Moreira, D. M., Talpe, M., 2025. Measuring river slope using spaceborne GNSS reflectometry: Methodology and first performance assessment. *Remote Sensing of Environment* 318, 114597. https://doi.org/10.1016/j.rse.2025.114597

Westerberg, I., Karlsen, R. H. 2024. Sharing perceptual models of uncertainty: On the use of soft information about discharge data. Hydrological Processes, 38(5). https://doi.org/10.1002/hyp.15145

WSDOT, 2025. *Hydraulics manual*, M23-03.11. Washington State Department of Transportation, Olympia, WA.

Yu, C.-W., Hodges, B. R., Liu, F., 2020. A new form of the Saint-Venant equations for variable topography. *Hydrology and Earth System Sciences* 24, 4001–4024. https://doi.org/10.5194/hess-24-4001-2020